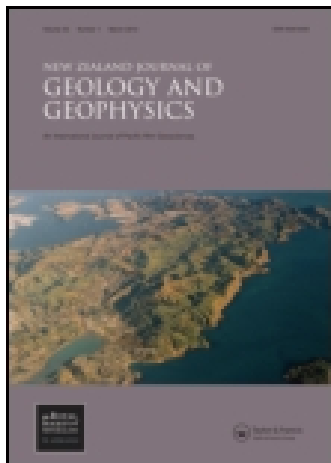


This article was downloaded by: [121.73.235.252]

On: 29 March 2015, At: 14:00

Publisher: Taylor & Francis

Informa Ltd Registered in England and Wales Registered Number: 1072954 Registered office: Mortimer House, 37-41 Mortimer Street, London W1T 3JH, UK



New Zealand Journal of Geology and Geophysics

Publication details, including instructions for authors and subscription information:

<http://www.tandfonline.com/loi/tnzg20>

Metal redistribution in historic mine wastes, Coromandel Peninsula, New Zealand

D. Craw^a & D. A. Chappell^a

^a Geology Department, University of Otago, P.O. Box 56, Dunedin, New Zealand

Published online: 23 Mar 2010.

To cite this article: D. Craw & D. A. Chappell (2000) Metal redistribution in historic mine wastes, Coromandel Peninsula, New Zealand, *New Zealand Journal of Geology and Geophysics*, 43:2, 187-198, DOI: [10.1080/00288306.2000.9514880](https://doi.org/10.1080/00288306.2000.9514880)

To link to this article: <http://dx.doi.org/10.1080/00288306.2000.9514880>

PLEASE SCROLL DOWN FOR ARTICLE

Taylor & Francis makes every effort to ensure the accuracy of all the information (the "Content") contained in the publications on our platform. However, Taylor & Francis, our agents, and our licensors make no representations or warranties whatsoever as to the accuracy, completeness, or suitability for any purpose of the Content. Any opinions and views expressed in this publication are the opinions and views of the authors, and are not the views of or endorsed by Taylor & Francis. The accuracy of the Content should not be relied upon and should be independently verified with primary sources of information. Taylor and Francis shall not be liable for any losses, actions, claims, proceedings, demands, costs, expenses, damages, and other liabilities whatsoever or howsoever caused arising directly or indirectly in connection with, in relation to or arising out of the use of the Content.

This article may be used for research, teaching, and private study purposes. Any substantial or systematic reproduction, redistribution, reselling, loan, sub-licensing, systematic supply, or distribution in any form to anyone is expressly forbidden. Terms & Conditions of access and use can be found at <http://www.tandfonline.com/page/terms-and-conditions>

Metal redistribution in historic mine wastes, Coromandel Peninsula, New Zealand

D. CRAW

D. A. CHAPPELL

Geology Department
University of Otago
P.O. Box 56
Dunedin, New Zealand

Abstract Mine wastes from historic gold mining on the western Coromandel Peninsula have variable base metal (Cu, Pb, Zn) contents, from near background (10–100 ppm) to several weight percent. Arsenic occurs as a minor element in some sulphide minerals, and is typically at c. 10% of the base metal levels in mine wastes. Decomposition of primary sulphide minerals is slow because the moist climate keeps the wastes saturated with water, so as to exclude oxygen, and alteration zones are on the millimetre scale after 100 years. Waters in the mine wastes have pH varying from 1.5 to 8, depending on host-rock composition and permeability to flushing rainwater. Carbonate-rich tailings can neutralise any acidity generated by sulphide oxidation. Without carbonate, pH drops due to pyrite decomposition. Iron oxyhydroxide from pyrite decomposition forms localised cements in mine wastes, and this cement incorporates some other metals. Base metals can be fixed in the iron oxyhydroxide at high pH (6–8), but arsenic is soluble and is flushed from the rock. At pH 2–4, base metals are largely flushed in solution, whereas arsenic is locally fixed in iron oxyhydroxide precipitates. Iron oxyhydroxide-rich spring precipitates (ferricrete) from the Monowai mine form at pH near 2, but co-precipitation of iron phosphate(s) and other phosphatic material incorporates dispersed metals, especially arsenic, which prevents their discharge into the environment.

Keywords Coromandel Peninsula; gold mining; mine tailings; environmental geochemistry; base metals; arsenic; ferricrete

INTRODUCTION

Old mining areas are well known for elevated metal concentrations in drainage waters (Chapman et al. 1983; Davis & Ashenberg 1989; Rampe & Runnels 1989; Webster et al. 1994; Plumlee et al. 1995). These metals are derived by leaching of mine excavations and solid mine wastes whose elevated metal contents and fine grain-sizes exposed to oxidation provide ready sources (Garrels & Thompson 1960; Nicholson et al. 1988; Davis & Ashenberg 1989). Most

environmental studies of such situations focus on the water, the dissolved metals, and their downstream attenuation, as these are of most immediate significance to the biosphere (Chapman et al. 1983; Davis & Ashenberg 1989; Kimball et al. 1995). Relatively little attention is paid to the mineralogical and geochemical processes occurring within the solid mine waste, except to define the contribution of pyrite breakdown to acid drainage and metal discharge (Garrels & Thompson 1960; Cherry et al. 1986; Nicholson et al. 1988; Moses & Herman 1991).

Coromandel Peninsula is a historic gold mining area in northern New Zealand, where underground mines were widely scattered in rugged forest country (Fig. 1A). The Tui mine tailings to the south of the peninsula (Fig. 1A) are notorious for their contribution of metals to the immediate drainage (Ward et al. 1977; Morrell et al. 1995; Pang 1995). Farther north on the Coromandel Peninsula, old mine wastes are a common but small part of the landscape. Rainfall is high (2–4 m/yr), so streams have a near-constant supply of runoff, and valleys are regularly flushed by floods. Hence, despite the widespread mine wastes, water quality is generally high and dissolved metal contents are commonly low (below New Zealand recommended maximum levels; Carter 1983; Beaumont et al. 1987). Nevertheless, the mine wastes are not inert, and they are undergoing constant geochemical and mineralogical changes *in situ*. This study describes the nature of a representative selection of mine waste sites and examines variations in mineralogy, geochemical environments, and metal contents seen at these sites. The selected sites provide useful information for comparisons of geochemical processes among the sites, and comparisons with mine wastes elsewhere in New Zealand and other humid climatic regions.

BACKGROUND

General geology

Coromandel Peninsula has a basement of Mesozoic greywacke which has been overlain and intruded by late Cenozoic igneous rocks, dominantly andesites and rhyolites (Williams 1974; Braithwaite et al. 1989; Adams et al. 1994) (Fig. 1A). These host rocks have been cut by structurally controlled hydrothermal vein systems which contain variable amounts of gold and base metals within quartz veins with common late-stage calcite (Williams 1974; de Ronde & Blattner 1988; Cargill et al. 1995). The host rock around vein systems is generally intensely altered to clays and/or sericite, and is flooded with quartz and pyrite (Rabone 1975; de Ronde & Blattner 1988; Braithwaite et al. 1989). Intensity of alteration falls off rapidly over 50–100 m, but weak propylitic alteration of host rocks to chlorite, epidote, sericite, and calcite persists over large volumes (tens to hundreds of cubic kilometres; Fig. 1B) (Rabone 1975; Merchant 1986; de Ronde & Blattner 1988; Braithwaite et

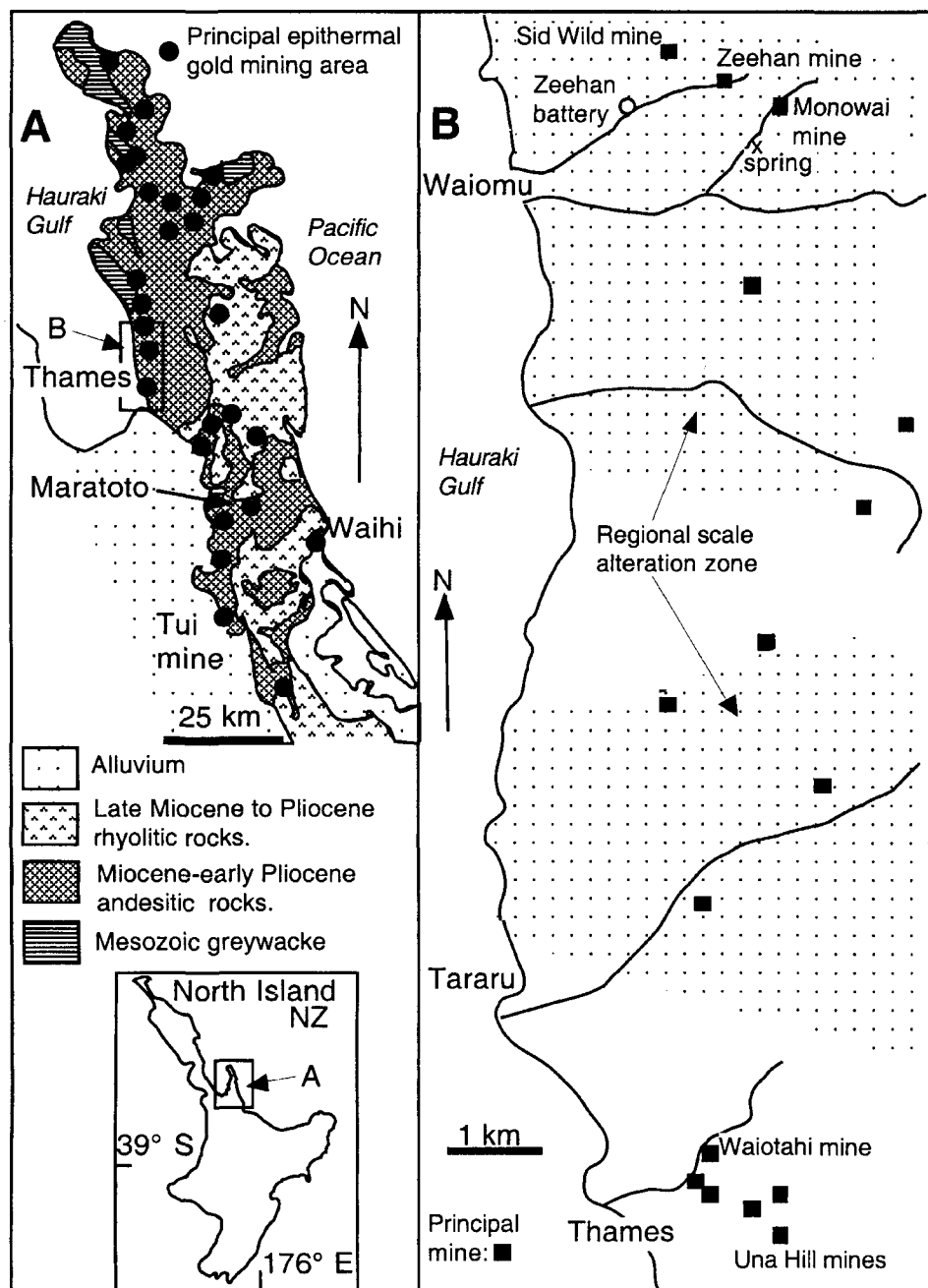


Fig. 1 **A**, Geological map of Coromandel Peninsula (after Williams 1974; Braithwaite et al 1989), showing the main rock types and the principal gold mining areas. **B**, Sketch map of the Thames-Waiomu portion of western Coromandel Peninsula (see box in A), showing the relative locations of most of the localities mentioned in the text. Regional scale hydrothermal alteration, mainly propylitic, is stippled (after Merchant 1986).

al. 1989). The high rainfall erodes less-resistant rock types rapidly, and this results in steep topography covered in dense forest in which outcrop is sparse away from streams, except in old mine workings. The present study examines old mine workings and tailings from processing plants near those workings, on the western side of the peninsula where the main host rock type is andesite (Fig. 1A).

Mining and processing practices

Gold commonly occurs in or near sulphide-rich portions of vein systems and in the altered host rocks. Consequently, historic miners of the pre-1960's era extracted the sulphide-rich material and associated quartz and altered host rock while following the vein structures underground. Extracted material with profitable gold grades was processed as ore,

and the rest of the extracted rock was dumped down hillsides at the entrances to the underground tunnels. The ore was transported to processing plants that were dominated by a crushing battery which reduced the ore to sand-sized particles. Fines from this process were washed downstream. Gold was extracted from the crushed ore by gravity settling, mercury amalgamation or cyanidation, and the residue was discharged as tailings into a nearby stream. Floods readily removed the sand down to the sea, and there is no sign of this material today except in the immediate vicinity of some batteries. In contrast, more modern (post-1960) mining practices involve mainly open-cut mining, producing a pit. Tailings from a processing plant after cyanidation are impounded behind a purpose-built dam, to isolate the tailings from the environment as much as possible.

SAMPLING AND ANALYTICAL METHODS

The end results of mining as outlined above are an excavation, either surface or underground; piles of waste rock which was not economic to process; and tailings from the processing plant, either residual (pre-1960) or fully impounded. In this study, we examine a range of sites to document the nature of processes occurring within solid waste material. We sampled material from waste rock dumps outside underground tunnels at numerous sites in the Thames-Waiomu area (Fig. 1A, B), residual tailings at Zeehan battery (Fig. 1B), a tailings impoundment at Maratoto (Fig. 1A), and precipitates from discharging water from an underground mining area (Monowai mine, Fig. 1B). Sampling consisted of extracting c. 100 g of material from

small (mainly <300 mm) pits dug into the waste material. Some small (50 mm scale) pieces of material remained intact when sampled due to *in situ* cementation, and this material was stored damp in sealed plastic bags until it could be dried, glued, and cut for thin-section examination in the laboratory. Sample splits were dried, crushed, and formed into pressed-powder disks for X-ray fluorescence (XRF) trace element analysis (Table 1), for comparison to typical background andesite levels of As = c. 10 ppm; Cu = c. 50 ppm; Zn = c. 70 ppm; Pb = c. 15 ppm (e.g., Patterson & Graham 1988; Wilson 1989). Selected distinct sample layers in old tailings were analysed for sulphur content with a Carlo-Erber elemental analyser using c. 10 mg charge, and carbonate content was determined using weight loss after addition of dilute HCl.

Table 1 Metal analyses for Coromandel mine wastes; all analyses are in ppm. Analyses were conducted by X-ray fluorescence spectrometry on pressed-powder pellets. Detection limit is c. 5 ppm, and analytical error is ±5 ppm below 200 ppm, ±10 ppm below 1000.

Sample	As	Ni	Cu	Zn	Pb	Sample	As	Ni	Cu	Zn	Pb	
Maratoto tailings						Zeehan battery tailings (continued)						
Hole						ZB10a	179	8	2157	4865	7598	
MTA1a	A	<5	14	12	68	33	ZB10a	85	6	792	1480	3808
MTA1b	A	<5	14	12	57	29	ZB10b	1969	84	75089	248243	
MTA2a	A	<5	17	11	126	44	ZB10c	39	<5	1658	6099	2603
MTA2b	A	5	19	14	147	48	ZB10Aa	119	<5	736	1071	4424
MTA3a	A	<5	17	16	133	48	ZB10Ab		<5	697	2100	4946
MTA3b	A	<5	20	12	161	46	ZB10Ac	119	5	585	408	4639
MTA3c	A	5	17	20	146	49	ZB10Ad	1104	66	33327	119894	
MTB1a	B	5	13	39	196	38	ZB10Ae	393	5	3469	8481	13965
MTB1b	B	<5	12	36	181	35	Zeehan mine waste dump					
MTB2a	B	<5	7	36	93	53	ZMWD/1a	71	26	264	1216	3364
MTB2b	B	5	14	50	166	43	ZMWD/1b	101	25	493	3143	5787
MTB2c	B	5	14	23	147	50	ZMWD/1c	62	36	558	2790	3862
MTB2d	B	6	23	28	95	55	ZMWD/2a	38	56	172	150	168
MTC1a	C	8	17	20	130	55	ZMWD/2b	57	48	172	157	207
MTC1b	C	<5	24	15	79	32	ZMWD/2c	57	48	172	161	204
MTD1a	D	<5	14	29	144	70	ZMWD/3a	101	42	238	513	1567
MTD1b	D	<5	12	37	154	70	ZMWD/3b	209	65	280	426	2212
MTE1a	E	8	22	24	130	53	ZMWD/3c	174	52	277	737	2588
MTE1b	E	7	26	29	124	55	Monowai mine waste dump					
MTJ1a	J	5	20	19	110	40	MWMD1a	40	27	34	271	926
MTJ1b	J	7	22	21	99	69	MWMD1b	37	18	23	189	763
MTJ1c	J	8	37	36	210	113	MWMD2a	171	18	41	187	261
Zeehan battery tailings						ZB3a	357	26	2988	743	11735	
ZB3b		459	18	3137	1506	12985	ZB3c	698	10	1483	7618	12505
ZB4a		5855	47	51720	513083	104487	ZB4b	709	12	2757	8131	13095
ZB4c		2462	77	64985	222339	73421	ZB4d	155	<5	433	660	3738
ZB4e		785	8	1863	8204	12873	ZB4e	785	8	1863	8204	12873
ZB5a		3115	289	72603	221124	55167	ZB5a	3115	289	72603	221124	55167
ZB5b		2413	12	2768	8165	3600	ZB5b	2413	12	2768	8165	3600
ZB5c		314	12	517	410	2635	ZB5c	314	12	517	410	2635
ZB5d		384	6	408	1406	7037	ZB5d	384	6	408	1406	7037
ZB6a		131	10	684	7281	9412	ZB6a	131	10	684	7281	9412
ZB6b		255	<5	3278	8980	1121	ZB6b	255	<5	3278	8980	1121
ZB7a		147	6	555	735	29933	ZB7a	147	6	555	735	29933
ZB7b		2089	12	6070	40449	65477	ZB7b	2089	12	6070	40449	65477
ZB8a		2599	90	64341	233522	19076	ZB8a	2599	90	64341	233522	19076
ZB8b		358	<5	706	2109	78419	ZB8b	358	<5	706	2109	78419
ZB9a		1057	52	15189	54998	64153	ZB9a	1057	52	15189	54998	64153
ZB9b		197	8	581	1456	3839	ZB9b	197	8	581	1456	3839
ZB9c		141	<5	257	427	1674	ZB9c	141	<5	257	427	1674
ZB9d							ZB9d					
(continued)						MWMD3a						
						MWMD3b	79	16	58	686	1404	
						Monowai mine spring deposit						
						MW500/1a	353	6	22	92	8	
						MW500/1b	418	<5	19	63	13	
						MW500/1c	379	<5	20	70	10	
						MW500/2a	213	15	21	114	11	
						MW500/2b	252	6	21	93	7	
						MW500/2c	219	<5	23	145	11	
						MW500/3a	846	7	21	27	59	
						MW500/3b	741	10	28	26	34	
						MW500/3c	749	<5	30	27	47	
						MW500/4a	650	9	23	71	11	
						MW500/4b	518	25	18	117	13	
						MW500/4c	431	<5	26	186	9	
						MW500/5a	529	5	20	71	16	
						MW500/5b	472	20	21	91	16	
						MW500/5c	751	6	18	49	17	
						MW500/6a	29	31	34	118	22	
						MW500/6b	27	22	22	90	11	
						MW500/6c	12	18	77	77	8	

Measurement of pH and Eh in moist zones in sampling pit walls in mine waste rock and battery tailings was done with an Oakton WD35615 portable meter with combination pH and Eh electrode calibrated with standard pH solutions and Zobell's solution (Nordstrom 1977). These measurements generally involved packing moist material around the inserted electrode and gently vibrating the electrode to mobilise sufficient water to make an electronic connection. Eh and pH were measured in associated streams and waters also, for comparison to the wet or moist waste material.

The mine wastes described above have been left undisturbed in a wet climate for 30–100 yr. Since the mine wastes contain variable amounts of sulphide minerals which are unstable in oxidised water, some secondary mineralogical transformations and metal mobility are expected. Because of the short time-frame, the degree of transformation is not large, and most original sulphide minerals are still preserved. Secondary products of alteration of sulphide minerals are fine grained (micrometre scale), intimately intermixed, and mainly X-ray amorphous. Hence, it is difficult to characterise these materials mineralogically. To elucidate the chemistry of these secondary products, we have made extensive use of electron microprobe element mapping to resolve metal distribution and redistribution in secondary alteration zones.

The electron microprobe mapping techniques were carried out on a JEOL 8600 instrument. Microprobe maps were constructed using automated analysis of 2 m diameter spots on a 2 m grid pattern over selected areas of polished thin sections. Each spot analysis results from 0.1 s counting, using wavelength dispersion at 25 kV, and so results are semiquantitative only because of this short counting time. Background levels for the analysed metals vary from mineral to mineral and are highest over metallic minerals where background is typically 0.2–1.0 wt%. These background levels are confirmed by spot analyses with 100 s counting times over known metal-enriched points. Output from this technique is an element map with 2×2 m pixels shaded for different weight percent of the metal, with darker zones representing relatively high levels of the metal.

MONOWAI MINE AREA

The Monowai mine (Fig. 1B) is a set of tunnels which follow a vein system over c. 1 km on a northeast-trending steep hillside (Roberts 1989). The mine was active sporadically from the late 19th century, and extensively re-prospected in the 1970s and 1980s. Waste rock dumps extend c. 50 m downslope from tunnel entrances, and are c. 20 m wide. They are scattered through regrowth forest and are partially revegetated. The dumps are generally partially or wholly water-saturated below c. 50–100 mm from the surface, and some have active seepages emanating from their flanks. The waste rock is variably altered volcanic rock rich in clay, sericite, quartz, and pyrite. XRF trace element analyses (Table 1, Fig. 2A) show that the waste dump material is slightly enriched in As, Cu, Zn, and Pb over typical background levels (above).

Spring discharge precipitate

A spring emanates from the hillside c. 100 m below some entrances to the underground workings of the southern portion of the Monowai mine (Fig. 1B). This spring does not emanate from any known mine workings, and may be

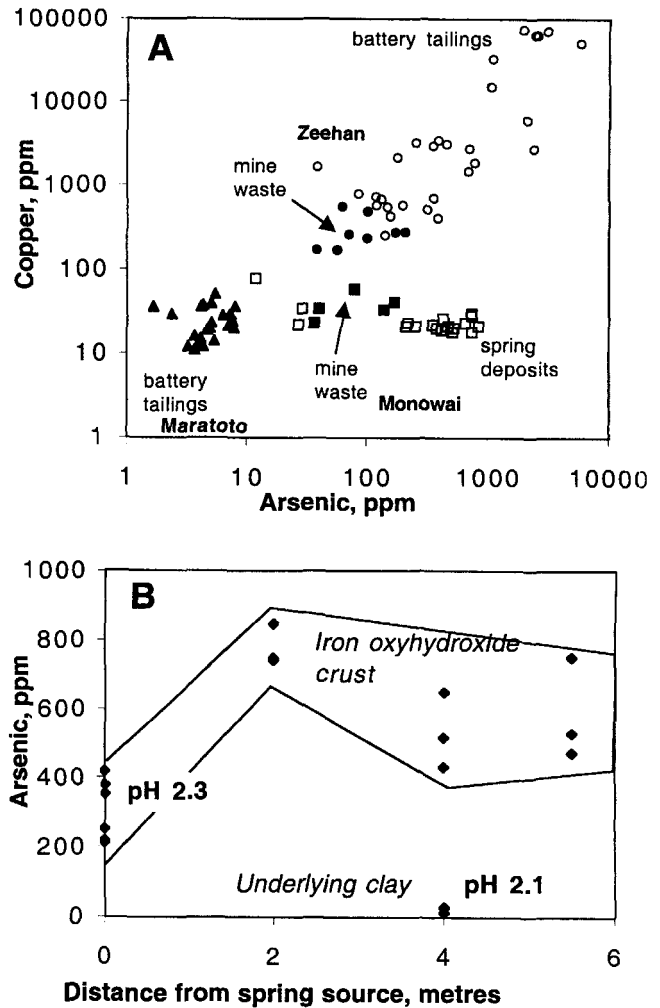


Fig. 2 Metal distribution in some Coromandel mine wastes. A. Copper and arsenic contents of mine wastes at Maratoto (triangles = tailings), Zeehan (filled circles = waste rocks, open circles = battery tailings), and Monowai mine (filled squares = waste dumps, open squares = spring precipitates). B. Arsenic content of Monowai spring precipitates with distance from the spring discharge point. Water pH of the discharging spring and saturated underlying clay are indicated.

natural in origin. The discharge waters flow over a clay soil surface for c. 8 m before dispersing into the soil and other surface drainage courses. Ferruginous precipitates (ferricretes) have formed on the surface where the water flows, and several small terraces (c. 1 m wide and 200 mm thick) have built up above the soil level. Some of the discharge waters flow over the top of the terraces, adding to their height with time. The present ferricrete terrace system has developed since a prospecting road was cut through the spring discharge site in the 1970s (Carter 1983).

Discharging water from the spring has pH near 2.3, and this water saturates the underlying clay zone which has pH of 2.1 (Fig. 2B), compared to saturated soil and stream water a few metres away which has pH of 6–7. XRF analyses of the ferricrete material (Table 1; Fig. 2A) show that it has low levels of trace elements except for elevated arsenic (up to c. 800 ppm). The arsenic levels are highest 2 m from the discharge point, but remain high to the downstream limit of the ferruginous terraces (Fig. 2B).

The Monowai mine spring ferricrete consists predominantly of iron oxyhydroxide, which is X-ray amorphous; no crystalline material is detectable. The precipitate has overgrown organic matter (mainly leaf litter and twigs), and the structure of the precipitate is dominated by casts of partially decayed organic material, which have been irregularly and imperfectly cemented by iron oxyhydroxide. Interstices are also locally filled with amorphous clay. Typical precipitate structure is displayed by the microprobe element maps presented as Fig. 3, particularly the iron map (Fig. 3A). In the latter map, part of a near-intact plant stem (curved, lower right) has been replaced and encrusted by iron oxyhydroxide with concentric rings. Other iron oxyhydroxide-rich parts (dark in Fig. 3A) have more irregular structure and are probably encrusting fragmental plant debris.

The phosphorus map (Fig. 3B) shows that iron oxyhydroxide is commonly accompanied by small but significant amounts of phosphorus, following the same structures. Small ringed areas in Fig. 3B highlight phosphate-rich fragments that have no iron. Sulphur is dispersed through the precipitate at low levels (<3 wt%; Fig. 3C), with highest levels commonly occurring where iron concentrations are highest. Because this material is all X-ray amorphous, no distinct mineral(s) intergrown with the iron oxyhydroxide can be identified. However, some metaliferous iron phosphate species are implied from the chemical data and paragenesis (cf. Pring et al. 1995; Ashley et al. 1997).

Metal concentrations in the ferricrete are generally proportional to the iron content (Fig. 3D–G). Some of this apparent proportionality is due to the higher analytical background levels over iron-rich material and is therefore an instrument artifact. This applies for the low-density patterns in Fig. 3D–G over iron-bearing patches, compared to the clear, iron-free patches (Fig. 3A), which are silicates or mounting resin, neither of which contain iron and both of which have low metal background levels. However, the higher density patterns in Fig. 3D–G are indicative of metal contents greater than detection limits (see Fig. 3, lower left corner). These metal maps show that there are small but significant amounts of metals dispersed through the iron oxyhydroxide matrix, mainly around the 1 wt% level. Small (10 μm scale) black spots on the copper map (Fig. 3D) suggest that discrete copper minerals have formed. These are not sulphides (Fig. 3C) and are assumed to be oxides or native copper. These spots are not resolvable with light microscopy, and so do not form discrete grains at the 10 μm scale. The arsenic map shows similar distributed metal concentrations as Cu, Pb, and Zn except that the iron-free phosphate material ringed in Fig. 3B locally contains relatively large amounts of As (c. 1.5 wt%). These As-rich patches are presumably rare as the bulk As content of the material is <1000 ppm (Table 1; Fig. 2A).

ZEEHAN MINING AREA

The Zeehan mine area lies immediately northwest of the Monowai mine (Fig. 1B) and consists of several sets of underground workings which were initiated in late 19th century and abandoned about 1912. We examined two waste dump sets, at the main Zeehan mine and the Sid Wild mine (Fig. 1B). These waste dumps are similar in size and content

to those of the Monowai mine (above), except that the Sid Wild waste is locally richer in clay than the other dumps, and forms soft grey-white ductile masses which are difficult to sample. The clays are readily washed out of the waste, and the top surfaces of the Sid Wild dumps are armoured with resistant quartz-rich clasts. Washed parts of the waste dumps have pH between 4 and 5. *In situ* pH measurements of saturated clay-rich wastes show that they are very acid, with pH between 1.5 and 2. Seepages with this pH emerge from the base of one waste pile into the adjacent stream whose pH is 6.5 upstream of the waste pile. The stream pH decreases to c. 4 (variable due to turbulence and partial mixing) for 3 m, then rises back to 6.5 over 2 m. Thin (micrometre scale) iron oxyhydroxide coatings on stream pebbles signal the pH mixing area.

Battery tailings

The Zeehan battery structure is still largely intact downstream of the underground workings (Fig. 1B), although nearly all the machinery has been removed. A tailings residue of bedded sand up to 200 mm thick remains on the 4 \times 5 m concrete floor of the battery discharge chute, and has remained undisturbed since the site was abandoned. Delicate planar layering (millimetre–centimetre scale) is preserved in these tailings, defined by differing proportions of sulphide minerals (Fig. 4), which represents processing of ore from different parts of the mine system. Some layers at the 1–10 mm scale are essentially sulphide mineral sands with little silicate material (Fig. 4). Individual layers are continuous for 1–5 m laterally and down-dip, but change in thickness, especially by thinning down-dip. Primary layering is visible in microscope sections at the millimetre scale, but bedding no longer appears planar (Fig. 4) due to compaction processes. Bedding boundaries at this scale are less sharp, especially for sulphide-rich layers, which have an iron oxyhydroxide cement zone c. 0.1–0.5 mm wide on their margins.

The tailings are moist but not all saturated with water, and pH measurements were made only on the wettest zones. It was not possible to determine pH of single layers, as the electrode width and measuring strategy (above) disturbed 10–20 mm of material. The measured pH sites and results for one pit in the tailings are shown in Fig. 4, and this general pattern is repeated in other pits. The pH in most of the tailings is near 5, but sulphide-rich layers (see %S data, Fig. 4) have pH near 2, and the pH rises to 6 near to the concrete substrate. The carbon dioxide content is <2.5 wt% in all analysed samples (Fig. 4).

Sulphur content of the tailings is locally high (up to 25 wt%; Fig. 4), confirming the visual observations that some layers are almost entirely sulphide sands, and sulphide minerals are common constituents of the tailings throughout the pile. The metal compositions of tailings samples reflect this high sulphide content and reach up to several percent copper, lead, and zinc (Table 1). Arsenic contents are lower than the base metals, but still reach almost 1 wt% in some samples (Table 1; Fig. 2A). There is a strong positive correlation between base metal content and arsenic content (Table 1; Fig. 2A), with arsenic content generally c. 10% of the copper content (Fig. 2A). The Zeehan mine and Monowai mine waste dump samples fit this same trend, at lower levels, reflecting the distinction made between ore and waste by the historic miners.

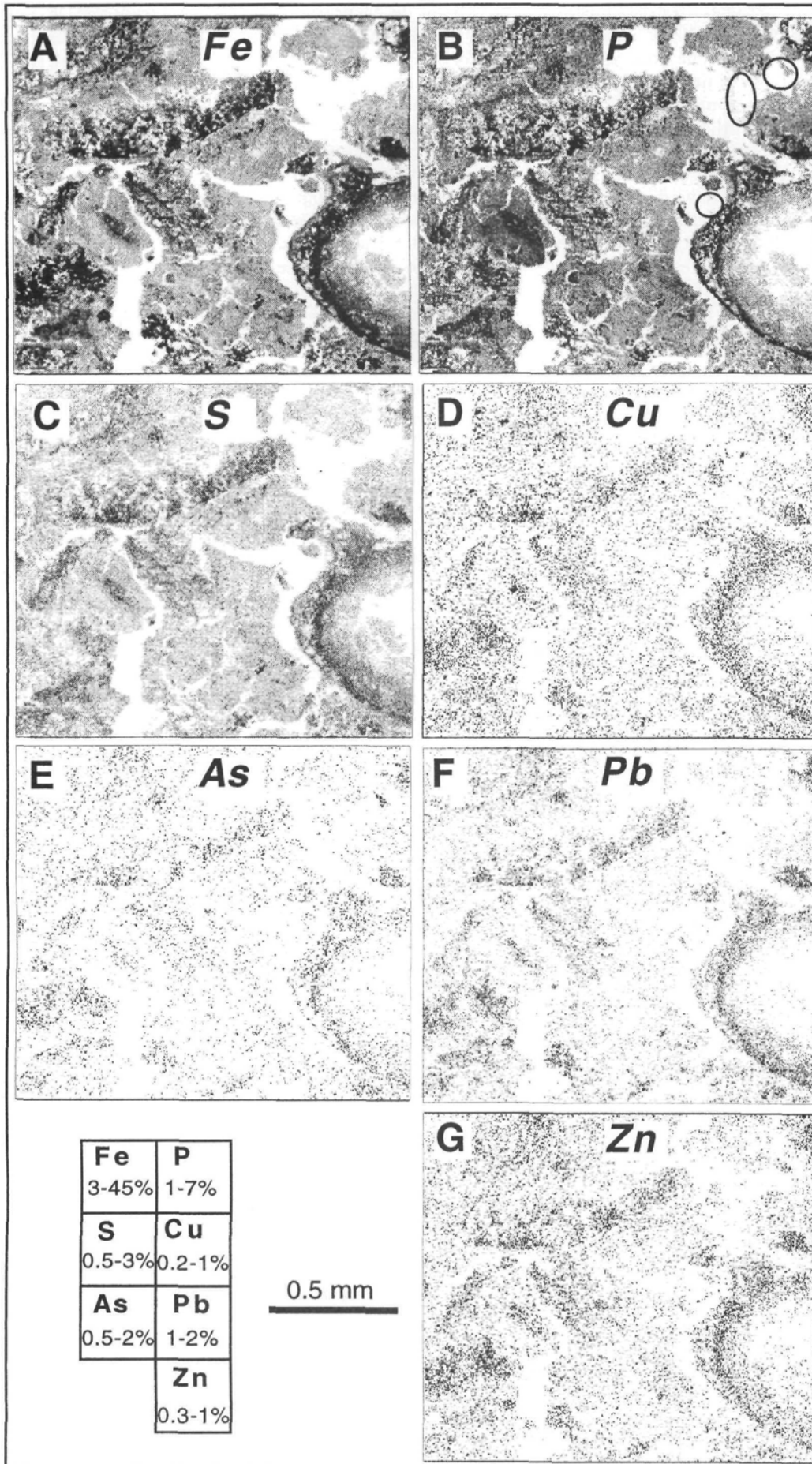
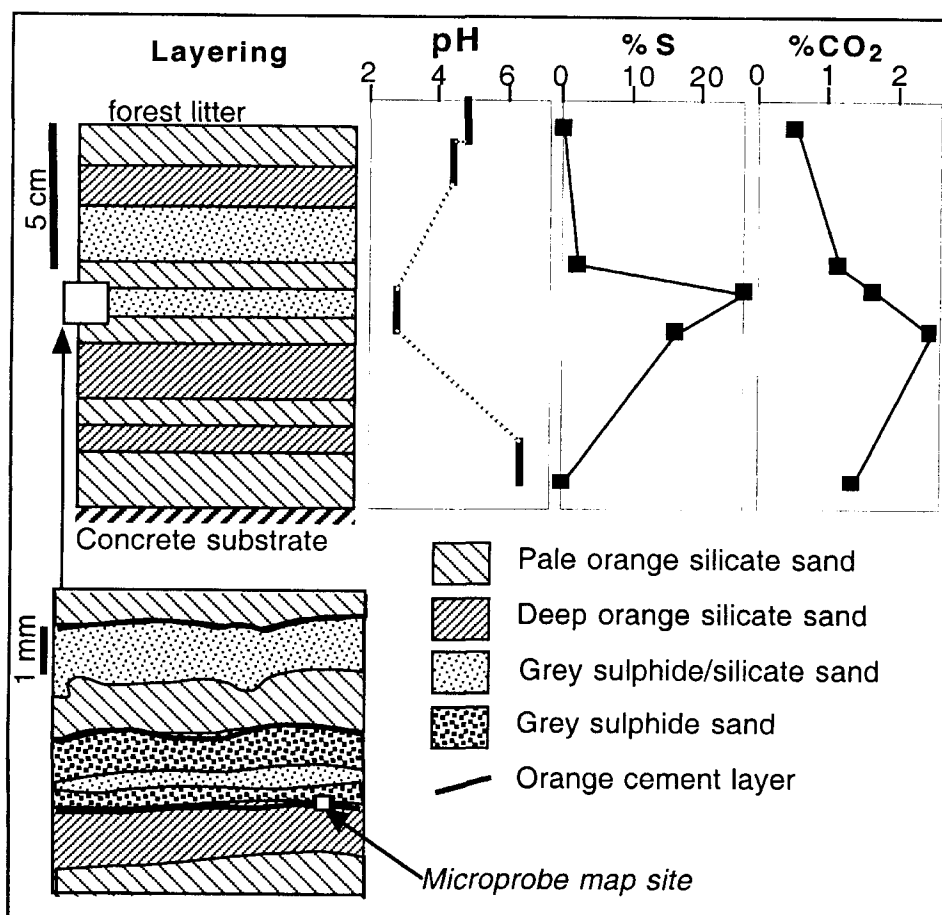


Fig. 3 Microprobe element maps (see text for methods) of a portion of a piece of Monowai mine area ferricrete. All maps are of the same area and show distributions of indicated elements, with concentration being proportional to darkness of the pattern on each map. Approximate ranges of concentrations of each element are indicated in the lower left corner: the lower number represents the detection limit, and the higher number represents the minimum concentration at the darkest spot on the map. Small ringed areas in B highlight phosphate-rich fragments that have no iron.

Fig. 4 Sketch of a measured section through a pit dug in 100 yr old tailings preserved on the floor of the Zeehan battery. The full section is shown at top left, with chemical data for samples from that section shown at top right. A map of a polished thin section across some sulphide-rich/silicate-rich layers (white box in main section) is shown at lower left, and the site of a microprobe map across a layer boundary (Fig. 5) is indicated in this thin-section map.



A set of microprobe maps (Fig. 5) was constructed across a delicate bedding boundary between sulphide-rich and limonitic silicate sand in Zeehan battery tailings (Fig. 4). This bedding boundary is intensely iron oxyhydroxide-stained and cemented, as observed in thin section (Fig. 4). The lower half of the map in Fig. 5 is the sulphide sand layer, as shown up by the iron-rich grains (Fig. 5A) and the sulphur-rich grains (Fig. 5E). Copper and zinc sulphides are also apparent (Fig. 5C, D, F), and lead-sulphur minerals such as galena (identified in polished sections) and/or anglesite (a common oxidation product in Coromandel; Williams 1974). Many of these sulphides contain arsenic (Fig. 5B; c. 1–10 wt%), presumably in solid solution with the main metals. The arsenic most commonly accompanies lead (Fig. 5F) in both sulphur-bearing and sulphur-free minerals (Fig. 5E).

The iron oxyhydroxide-stained bedding boundary is defined by the strong band of iron, without sulphur, in the upper part of the maps (Fig. 5A, E). This iron oxyhydroxide cements the silicate grains and a few of copper and zinc sulphide grains (Fig. 5C, D). The pervasively cemented layer is only c. 50 μm thick, and minor iron oxyhydroxide fills grain interstices beyond the cemented layer in the silicate sand (Fig. 5A). Arsenic is present at slightly above background levels (c. 0.5 wt%) in the iron oxyhydroxide-cemented zone at the bedding boundary, forming an arsenic-rich band (Fig. 5B). Arsenic also accompanies iron oxyhydroxide in the silicate sand, but this is at near-background levels.

MARATOTO TAILINGS

The Maratoto mine (Fig. 1A) exploited quartz-rich veins and clay-bearing quartzofeldspathic host rock, and was last active in the 1960s. The processing plant was 5 km closer to Thames, on a river valley floor, and the tailings were discharged to a small impoundment behind a 5 m high dam (Fig. 6) on the valley side. A thin (centimetre-scale) surface layer of rock-crushing fines was added when the battery was re-used as a road aggregate plant. The mine tailings are sand-sized grains of mainly quartz and feldspar. They are weakly bedded on the millimetre scale, with thin (<10 mm) sulphide-rich layers occurring sporadically through the pits to within 150 mm of the surface. Coarser scaled bedding (100 mm scale) is defined by sulphide-bearing and sulphide-poor iron oxyhydroxide-bearing layers (Fig. 6). Layers are discontinuous on the 2–3 m scale, and correlation of individual layers from pit to pit (Fig. 6, 7) is difficult or impossible.

The tailings are fully saturated with water at the upstream end (south; Fig. 6) where a swamp has formed as the impoundment has interfered with the natural drainage. The tailings are saturated with water below c. 0.5–1.0 m, with the saturation level becoming deeper downslope (to the north; Fig. 6, 7). Surface water lies on the tailings in several places, perched on the cap of gravel-crushing fines. Almost all waters have neutral or alkaline pH except for the swamp, which has essentially no chemical interaction with the tailings (Fig. 6). The alkaline pH reflects the high carbonate content of the tailings, typically 7–8 wt% CO_2 (Fig. 7).

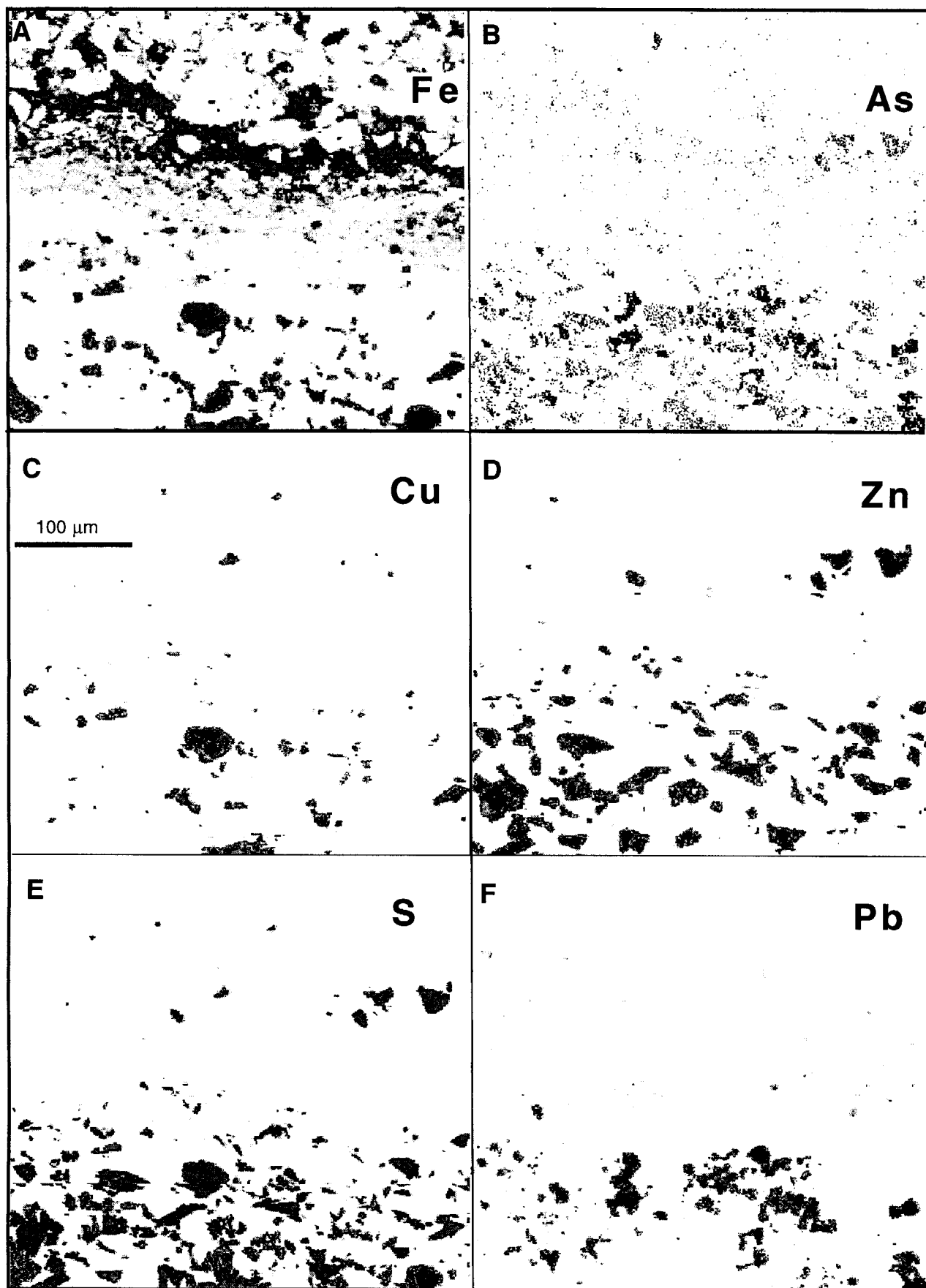


Fig. 5 Microprobe element maps across an oxidised sulphide-rich/silicate-rich layer boundary in Zeehan battery tailings (Fig. 4). Iron oxyhydroxide from oxidised pyrite forms a cement around silicate grains and forms a dark band across the iron map (A). A weak arsenic band, barely above background, follows this iron band in B. Primary sulphide minerals are shown up by base metal and sulphur maps (C–F).

Fig. 6 Map of the Maratoto tailings dam (with pecked ornament) and impounded tailings (stippled). Diverted drainage (heavy lines) goes around the impoundment and forms a swamp at their intersection. Contours, in metres above sea level, show the vertical scale. Water and moist tailings pH data are indicated at measurement sites. A line of vertical sections through the tailings is shown from A to C (see Fig. 7).

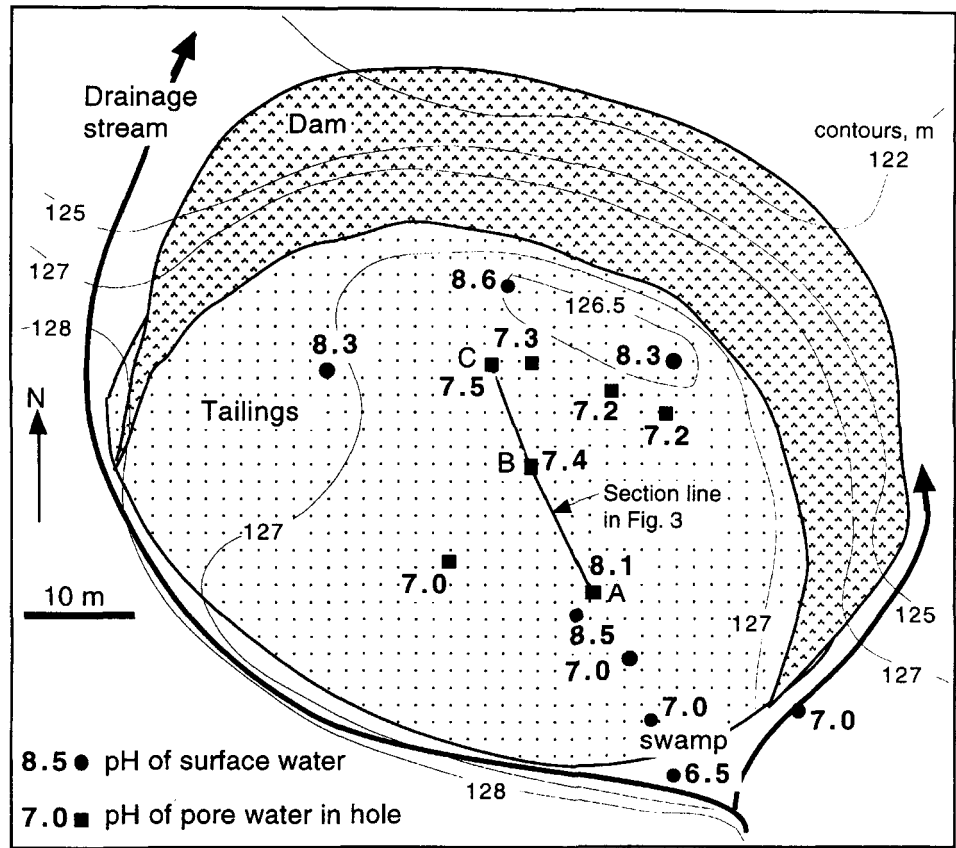
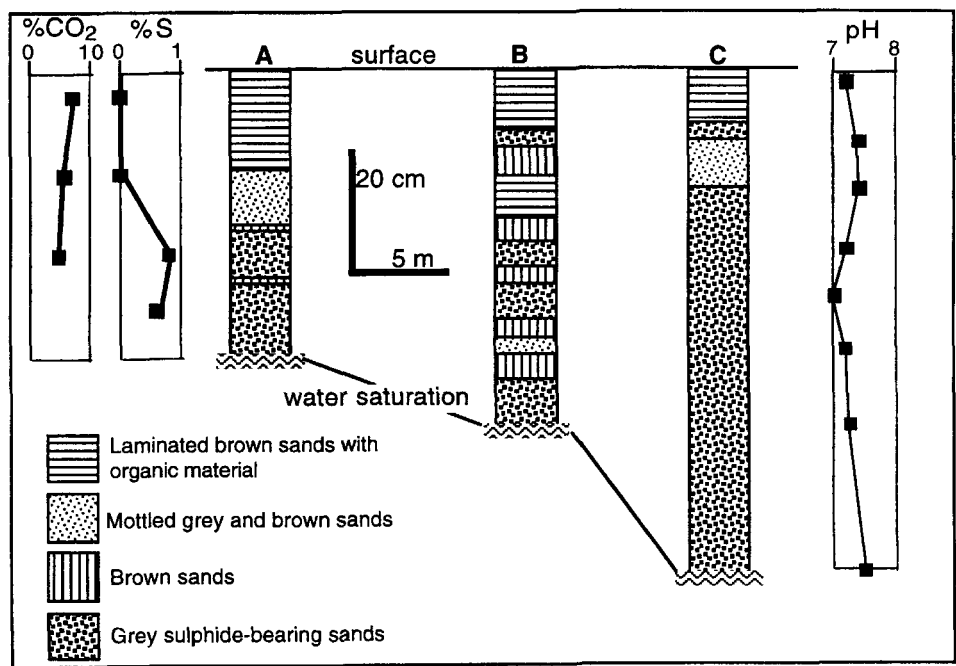


Fig. 7 Measured sections down pits dug in the Maratoto tailings to the water saturation level, at sites shown in Fig. 6. Note different vertical and horizontal scales. Carbon dioxide and sulphur analyses down pit A are shown on the left, and pH measurements down pit C are shown on the right.



The Maratoto tailings have generally lower sulphide mineral contents than those at the Zeehan mine waste and tailings, and sulphur concentrations are low (<1 wt%; Fig. 7). Likewise, the metal concentrations are at or near background levels in most samples (Table 1; Fig. 2A). The Maratoto tailings metal data fall on the same copper versus arsenic

trend as the Zeehan mine waste and tailings, but at the lower end (Fig. 2A).

There is little evidence of *in situ* alteration of the Maratoto tailings, other than thin seams of iron oxyhydroxide which cut across bedding and locally cement the sands in sulphide-bearing layers. These seams are <1 mm wide and

Downloaded by [121.73.235.252] at 14:00 29 March 2015

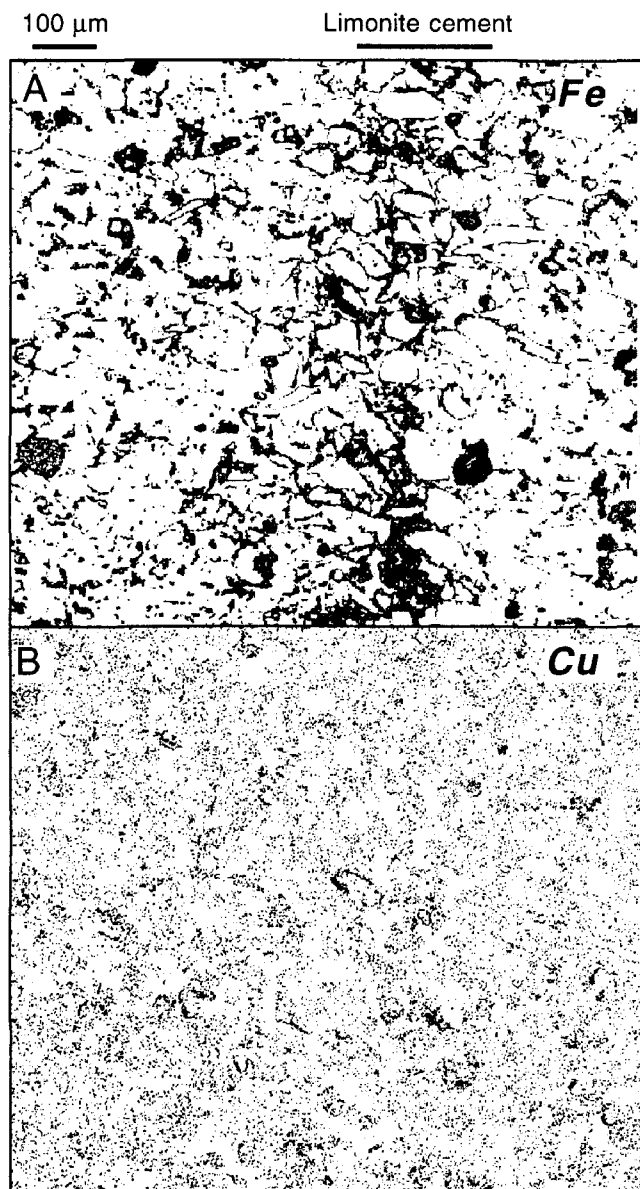


Fig. 8 Microprobe element maps of an oxidised seam in a sample from 200 mm from the top of pit A in Fig. 7. The seam is dominated by iron oxyhydroxide (dark zone in A) cementing silicates in the tailings in a zone at a high angle to bedding. Minor iron oxyhydroxide extends along grain boundaries across the whole map. Pyrite grains are dark in A. Copper map (B) shows localised concentrations of copper in cement, especially in the iron oxyhydroxide-rich seam. Most copper signal is too close to background to show a clear structure.

continuous for a few centimetres only. The structure of one of these seams is shown in Fig. 8A, an iron microprobe map. The dark zones on this map represent high iron concentrations, and white represents iron-free silicates. The iron oxyhydroxide-cemented seam trends near-vertically across the map, as indicated. In this seam, iron oxyhydroxide surrounds and cements the silicate grains. Degree of cementation decreases to the left and right but persists right across the map. Scattered pyrite appears as dark grains; for example, several small grains are near the lower right map edge, and a large grain is below centre at the left edge.

Copper levels are near to background in the same map area, so patterns are difficult to resolve (Fig. 8B). However, there is a close correspondence between the highest copper levels (darkest patches) and iron oxyhydroxide cement in the iron oxyhydroxide seam (right of centre). One copper-rich zone near the centre of the map largely encircles a silicate grain and forms part of the cement. There are no chalcopyrite grains visible in this map, as confirmed by a sulphur map (not reproduced here).

THAMES MINING AREA

The Thames mining area involved exploitation of well-defined quartz veins with local bonanza gold concentrations. Many mine excavations are now exposed as underground workings, shallow tunnels, or quarries, although these are commonly dry. Groundwater drains from the host rock-mass and is chemically affected by that rock, so that surface seepages reflect the chemistry of the immediate host rock. Water emanating from propylitically altered andesites on Una Hill (Fig. 1B) is alkaline due to the calcite which is part of the alteration mineral assemblage. In contrast, water issuing from pyritic altered rock near mineralised zones on Una Hill and Waitotahi mine (Fig. 1B) is acidic, with pH as low as 2. Micrometre-scale iron oxyhydroxide precipitates coat stream sediments downstream of these sites for up to 3 km. More detailed mapping of these phenomena is described by Craw & Chappell (1998). Since there are no thick precipitates from these waters, they are not discussed further in this study, other than providing a geochemical baseline for host-rock control on groundwater chemistry.

DISCUSSION

Controls on pH

The pH of mine wastes is controlled by the immediate mineralogy of the host material, as outlined for groundwater seeps at Thames (above; Craw & Chappell 1998). Most Coromandel wastes contain substantial pyrite, and oxidation of pyrite results in acidification of waters (Garrels & Thompson 1960), so pH between 2 and 5 is typical of waste waters (Fig. 9) (Craw & Chappell 1998). This can be modified by incursion and dilution by rain or stream water, so permeability of waste material plays an important part in final pH of wastes. The Sid Wild wastes provide an extreme example, where impermeable pyrite-bearing clays prevent significant dilution. The pH has evolved to be so acid that ferrous iron is dominant, and brown iron oxyhydroxide is absent (Fig. 9). Some layers in the Zeehan battery tailings have undergone similar, although less extreme, chemical evolution. At the other end of the observed pH spectrum, Maratoto tailings (pH near 7) have high carbonate content and relatively low sulphide content (Fig. 7), so that any acid generated by pyrite oxidation is rapidly neutralised, and pH is maintained near neutral (Fig. 7, 9).

Metal fixation in mine wastes

Metals are fixed in the mine wastes primarily by the slow rate of reaction of the metal-bearing sulphides. After c. 100 years, sulphides in the Zeehan battery tailings are essentially unaltered and porewater chemistry has evolved almost to equilibrium with sulphides (Fig. 4, 9). This situation is

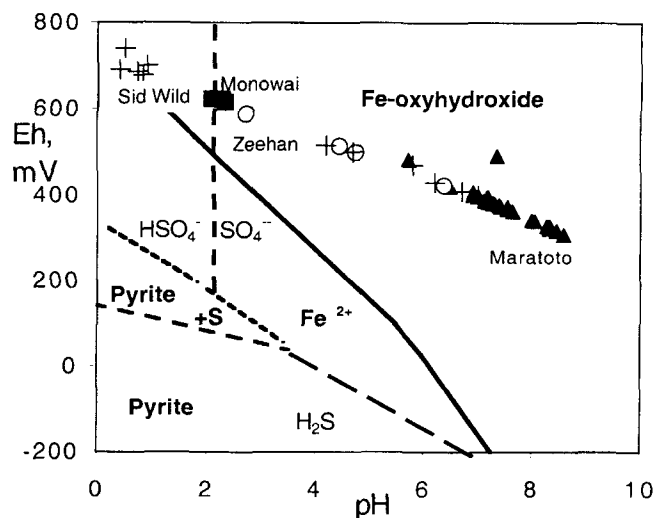


Fig. 9 Eh-pH diagram, showing the spread of measured data in Coromandel mine wastes: Maratoto tailings are filled triangles; Zeehan mine waste dumps and the Zeehan battery is open circles; Sid Wild mine waste dumps are crosses; and the Monowai mine spring is filled squares. Theoretical mineral stability boundaries, assuming maximum dissolved iron is 10–6 moles/litre, are calculated from Garrels & Christ (1965) and Wagman et al. (1982).

disturbed only where the sulphides lie adjacent to porous and permeable silicate sands, which have allowed chemical conditions to remain more oxidised and nearer to neutral. Even under these conditions, the sulphides show little evidence of alteration. Clearly, the wet climate provides sufficient moisture to ensure almost constant saturation and effective exclusion of oxygen (cf. Pang 1995). However, where the Zeehan tailings sulphides have become oxidised, copper, lead, and zinc are readily removed in solution and are not adsorbed or precipitated with iron oxyhydroxide (Fig. 5C, D, F). Only arsenic, a minor element in the sulphides, remains with the iron oxyhydroxide (Fig. 5B) to a limited extent, probably because it forms scorodite, which has relatively low solubility under moderately acid conditions (Krause & Ettl 1988), or is adsorbed on to iron oxyhydroxides.

Conversely, although metal contents are low in the Maratoto tailings (Fig. 2A), copper is partially retained during incipient oxidation (Fig. 8B). This difference is due to the higher pH of the tailings, which is maintained by the high carbonate content (Fig. 7). Copper is co-precipitated with iron oxyhydroxide (cf. Hem 1977; Chapman et al. 1983) as part of the cement. Arsenic, which is present at low but detectable levels in the sulphide minerals at Maratoto, is lost in solution when sulphides oxidise because of the high solubility of oxidised arsenic salts (Krause & Ettl 1988; Vink 1996).

Metals are fixed in the Monowai spring ferricrete to a surprising extent, considering the low pH of the fluid from which the precipitates form. This pH, near 2 (Fig. 2B), is similar to that prevailing in oxidising sulphides at the Zeehan battery (Fig. 4), where most metals have been flushed from the oxidised wastes. Arsenic, which leaves only a subtle residue in the Zeehan tailings iron oxyhydroxide (Fig. 5B), is strongly retained in the Monowai ferricrete (Fig. 2B, 3E), up to >800 ppm (Table 1). Retention of arsenic in these

precipitates is more pronounced than retention of copper, lead, and zinc (Fig. 2B; Table 1), which are near-background in bulk samples (Table 1) but locally elevated in iron oxyhydroxide (Fig. 3). Enhanced metal retention in the Monowai ferricrete at low pH is almost certainly due to formation of iron phosphate compound(s) and other phosphatic material (Fig. 3B), which readily incorporate metals (Pring et al. 1995; Ashley et al. 1997). The source of the phosphate to form these compounds is not known, but it may have combined inorganic (rock apatite) and organic (shallow soil and vegetation) sources. Clearly, formation of this phosphatic material is an important control on metal availability in the environment, particularly for arsenic.

CONCLUSIONS

Mine wastes in the Coromandel area have a wide range of base metal (Cu, Pb, Zn) contents, from near-background levels in quartzofeldspathic material, to strongly enriched (percent level). Arsenic is present at c. 10% of the base metal contents. Ferricrete precipitates from a spring derived from the Monowai mine area are relatively enriched in arsenic compared to base metal contents. These metals are variably mobilised during oxidation, and are locally retained with iron oxyhydroxide cements formed during decomposition of pyrite. Base metal retention in iron oxyhydroxide cements is enhanced at high (neutral) pH, which is maintained by high carbonate content in the primary ore, whereas arsenic is flushed from this material. Lower pH (2–4) favours flushing of base metals and retention of arsenic with iron oxyhydroxide. However, formation of phosphate compound(s) at pH near 2 in ferricrete apparently results in incorporation of metals, especially arsenic, and enhances metal retention *in situ*. Very low pH (<2) and low redox conditions prevail in some wastes, and these conditions require low permeability to resist incursion of rainwater.

Decomposition of sulphides in Coromandel mine wastes is slow, and results in only millimetre-scale alteration zones over 100 years. The combination of slow decomposition, localised incorporation of metals into iron oxyhydroxide cements, low permeability, and almost constant water saturation in a moist climate ensures that metal discharges into the environment from mine wastes in the Coromandel area are generally at low levels.

ACKNOWLEDGMENTS

This study was financed by the New Zealand Public Good Science Fund (Contract UOO620) and the University of Otago. We appreciate the expert assistance of S. Middlemiss, D. Walls, M. Trinder, and B. Pooley. Discussions with J. Webster and R. Braithwaite were useful and helpful. The Department of Conservation kindly permitted access for sampling on their estate. Constructive reviews by P. Ashley and R. Stewart improved the manuscript.

REFERENCES

- Adams, C. J.; Graham, I. J.; Seward, D.; Skinner, D. N. B. 1994: Geochronological and geochemical evolution of late Cenozoic volcanics in the Coromandel Peninsula, New Zealand. *New Zealand Journal of Geology and Geophysics* 37: 359–379.

- Ashley, P. M.; Lottermoser, B. G.; Scott, K. M. 1997: Supergene iron phosphate minerals in Proterozoic ironstones from the Olary Block, South Australia. *Neues Jahrbuch für Mineralogie Monatshefte*: 309–327.
- Beaumont, H. M.; Tunnicliffe, J. C.; Stevenson, C. D. 1987: Heavy metal survey of Coromandel streams. *Water and Soil Miscellaneous Publication 104*: 17–47.
- Braithwaite, R. L.; Christie, A. B.; Skinner, D. N. B. 1989: Hauraki goldfields: regional setting, mineralisation and recent exploration. In: Kear, D. ed. *Mineral deposits of New Zealand. Australasian Institute of Mining and Metallurgy Monograph 13*: 45–56.
- Cargill, H. J.; Christie, A. B.; Braithwaite, R. L.; Swain, A. 1995: Comparison of vein styles and distributions between rhyolite and andesite hosted epithermal gold-silver deposits of the Hauraki goldfield. In: Mauk, J. L.; St George, J. D. ed. *Proceedings, 1995 PACRIM Congress, Australasian Institute of Mining and Metallurgy, Parkville, Victoria, Australia*. Pp. 101–106.
- Carter, D. A. 1983: Heavy metal survey in the Coromandel. A case study in design of water quality surveys. *Water and Soil Miscellaneous Publication 63*.
- Chapman, B. M.; Jones, D. R.; Jung, R. F. 1983: Processes controlling metal ion attenuation in acid mine drainage streams. *Geochimica et Cosmochimica Acta 47*: 1957–1973.
- Cherry, J. A.; Morel, F. M. M.; Rouse, J. V.; Schnoor, J. L.; Wolman, M. G. 1986: Hydrogeochemistry of sulfide and arsenic rich tailings and alluvium along Whitewood Creek, South Dakota. *Mineral and Energy Resources 29*: 1–15.
- Craw, D.; Chappell, D. A. 1998: Hydrothermal controls on environmental metal mobility: a comparison between Otago and Coromandel. *Proceedings of the Australasian Institute of Mining and Metallurgy, New Zealand Branch Conference*. Pp. 48–58.
- Davis, A.; Ashenberg, D. 1989: The aqueous geochemistry of the Berkeley Pit, Butte, Montana, U.S.A. *Applied Geochemistry 4*: 23–36.
- de Ronde, C. E. J.; Blattner, P. 1988: Hydrothermal alteration, stable isotopes and fluid inclusions of the Golden Cross epithermal gold-silver deposit, Waihi, New Zealand. *Economic Geology 83*: 895–917.
- Garrels, R. M.; Christ, C. L. 1965: *Solutions, minerals and equilibria*. New York, Harper and Row.
- Garrels, R. M.; Thompson, M. E. 1960: Oxidation of pyrite in iron sulfate solutions. *American Journal of Science 258-A*: 57–67.
- Hem, J. D. 1977: Reactions of metal ions at surfaces of hydrous iron oxide. *Geochimica et Cosmochimica Acta 41*: 527–538.
- Kimball, B. A.; Callendar, E.; Axtmann, E. V. 1995: Effects of colloids on metal transport in a river receiving acid mine drainage, upper Arkansas River, Colorado, U.S.A. *Applied Geochemistry 10*: 285–306.
- Krause, E.; Ettel, V. A. 1988: Solubility and stability of scorodite, $\text{FeAsO}_4 \cdot 2\text{H}_2\text{O}$: new data and further discussion. *American Mineralogist 73*: 850–854.
- Merchant, R. 1986: Mineralization in the Thames district, Coromandel Peninsula. In: Henley, R. W.; Hedenquist, J. W.; Roberts, P. J. ed. *Guide to the active epithermal (geothermal) systems and precious metal deposits of New Zealand. Monograph Series on Mineral Deposits 26*: 147–163.
- Morrell, W. J.; Gregg, P. E. H.; Stewart, R. B.; Bolan, N.; Horne, D. 1995: Potential for revegetating base metal tailings at the Tui Mine site, Te Aroha, New Zealand. In: Mauk, J. L.; St George, J. D. ed. *Proceedings, 1995 PACRIM Congress, Australasian Institute of Mining and Metallurgy, Parkville, Victoria, Australia*. Pp. 395–400.
- Moses, C. O.; Herman, J. S. 1991: Pyrite oxidation at circumneutral pH. *Geochimica et Cosmochimica Acta 55*: 471–482.
- Nicholson, R. V.; Gilham, R. W.; Reardon, E. J. 1988: Pyrite oxidation in carbonate-buffered solution: 1. Experimental kinetics. *Geochimica et Cosmochimica Acta 52*: 1077–1085.
- Nordstrom, D. K. 1977: Thermochemical redox equilibria of ZoBell's solution. *Geochimica et Cosmochimica Acta 41*: 1835–1841.
- Pang, L. 1995: Contamination of groundwater in the Te Aroha area by heavy metals from an abandoned mine. *Journal of Hydrology (New Zealand) 33*: 17–34.
- Patterson, D. B.; Graham, I. J. 1988: Petrogenesis of andesitic lavas from Mangatepopo valley and upper Tama Lake, Tongariro Volcanic Centre, New Zealand. *Journal of Volcanology and Geothermal Research 35*: 17–29.
- Plumlee, G. S.; Smith, K. S.; Mosier, E. L.; Ficklin, W. H.; Montour, M.; Briggs, P.; Meier, A. 1995: Geochemical processes controlling acid-drainage generation and cyanide degradation at Summitville. In: Posey, H. H.; Pendleton, J. A.; Van Zyl, D. ed. *Proceedings, Summitville Forum. Colorado Geological Survey Special Publication 38*: 23–34.
- Pring, A.; Birch, W. D.; Dawe, J.; Taylor, M.; Deliens, M.; Walenta, K. 1995: Kintoreite, $\text{PbFe}_3(\text{PO}_4)_2(\text{OH}, \text{H}_2\text{O})_6$, a new mineral of the jarosite-alunite family, and lusungite discredited. *Mineralogical Magazine 59*: 143–148.
- Rabone, S. D. C. 1975: Petrography and hydrothermal alteration of Tertiary andesite-rhyolite volcanics in the Waitekauri valley, Ohinemuri, New Zealand. *New Zealand Journal of Geology and Geophysics 18*: 239–258.
- Rampe, J. J.; Runnells, D. D. 1989: Contamination of water and sediment in a desert stream by metals from an abandoned gold mine and mill, Eureka District, Arizona. *Applied Geochemistry 4*: 445–454.
- Roberts, P. J. 1989: Geology and mineralisation of the Monowai mine, Coromandel Peninsula. In: Kear, D. ed. *Mineral deposits of New Zealand. Australasian Institute of Mining and Metallurgy Monograph 13*: 59–61.
- Vink, B. W. 1996: Stability relations of antimony and arsenic compounds in the light of revised and extended Eh-pH diagrams. *Chemical Geology 130*: 21–30.
- Wagman, D. D.; Evans, W. H.; Parker, V. B.; Schumm, R. H.; Halow, I.; Bailey, S. M.; Churney, K. L.; Nuttall, R. L. 1982: The NBS tables of chemical thermodynamic properties. *Journal of Physical and Chemical Reference Data 11, Supplement 2*.
- Ward, N. I.; Brooks, R. R.; Roberts, E. 1977: Contamination of pastures by a New Zealand basemetal mine. *New Zealand Journal of Science 20*: 413–419.
- Webster, J. G.; Nordstrom, D. K.; Smith, K. S. 1994: Transport and natural attenuation of Cu, Zn, As, and Fe in the acid mine drainage of Leviathan and Bryant Creeks. In: Alpers, C. N.; Blowes, D. W. ed. *Environmental geochemistry of sulphide oxidation. American Chemical Society Symposium Series 550*: 244–260.
- Williams, G. J. 1974: *Economic geology of New Zealand. Australasian Institute of Mining and Metallurgy Monograph 4*.
- Wilson, M. 1989: *Igneous petrogenesis*. London, Chapman & Hall.